Comparative in Situ DRIFTS-MS study of12CO- And 13CO-TPR on CuO/Cep2 catalyst

ARTICLE *in* THE JOURNAL OF PHYSICAL CHEMISTRY C · JUNE 2009

Impact Factor: 4.77 · DOI: 10.1021/jp9020504

4 AUTHORS, INCLUDING:

Parthasarathi Bera
National Aerospace Laboratories
95 PUBLICATIONS **2,445** CITATIONS
SEE PROFILE

Aitor Hornes
IREC Catalonia Institute for Energy Research
21 PUBLICATIONS **474** CITATIONS
SEE PROFILE

Comparative in Situ DRIFTS-MS Study of ^{12}CO- and ^{13}CO-TPR on CuO/CeO_2 Catalyst

Parthasarathi Bera, Antonio López Cámara, Aitor Hornés, and Arturo Martínez-Arias*

Instituto de Catálisis y Petroleoquímica, CSIC, C/ Marie Curie 2, Campus de Cantoblanco, 28049 Madrid, Spain

Received: March 6, 2009; Revised Manuscript Received: April 27, 2009

A ceria-supported copper oxide catalyst has been examined with respect to interaction with CO by means of CO-TPR tests employing a DRIFTS cell as reactor. Parallel analysis of isotopic shifts in the DRIFTS spectra obtained upon interaction of the catalysts with either ^{12}CO or ^{13}CO allows unambiguous assignment of the various carbonyl and carbonate-type species formed. The study is complemented by separate examination of the stability of carbonyl species focused to get hints on the nature of CO adsorption centers at the catalyst surface. Joint analysis of gases evolution during the CO-TPR tests and DRIFTS spectra is employed to determine the nature of processes taking place during such tests. Additionally, analysis of the various CO_2 isotopes evolving during the course of a TPO run subsequent to ^{13}CO-TPR test is employed to discard the occurrence of CO disproportionation upon interaction of the catalyst with CO up to 400 °C.

Introduction

Catalysts of copper oxide dispersed on ceria are active for several reactions of technological interest involving CO such as preferential CO oxidation (CO PROX), water gas shift (WGS) reaction, and CO oxidation, and they are very interesting from an economical point of view in comparison with catalysts based on dispersed noble metals typically employed for these processes.[1−3] In this respect, it is important to study the nature of the interaction of CO with CuO/CeO_2, and one of the methods widely employed for this purpose is temperature programmed reaction employing CO as reductant (CO-TPR).[4] Although the method has proven useful to get hints on the nature of dispersed copper oxide species in this type of system, there are however many uncertainties during interpretation of redox processes responsible for the features detected in the classical CO-TPR tests performed over this type of catalyst. This is due to the possible simultaneous occurrence of different reactions like WGS and CO oxidation, and even in some case it has been proposed the occurrence of CO disproportionation (Boudouard reaction).[3−5] This poses difficulties to achieve catalytic−redox correlations on the basis of such tests.[6]

In order to get more precise information in this sense, on the basis of analysis of the evolutions of various carbonyls or carbonates that could be formed during the TPR test over this type of catalyst,[1,2] a diffuse reflectance infrared Fourier transform spectroscopy (DRIFTS) cell has been used as reactor and the corresponding spectra have been simultaneously recorded in the course of the TPR run. In turn, TPR of ^{12}CO has been compared with that of ^{13}CO to achieve a complete analysis of the species formed. In addition, such comparison aims also to solve doubts on the attribution of infrared bands appearing in this type of system upon interaction with CO since there exists the possibility of formation of a band attributed to a forbidden electronic transition in Ce^{3+}, which appears at frequencies around 2120 cm^{-1} typical for carbonyl species.[7,8] Supplementary temperature programmed oxidation (TPO) performed subsequently to the ^{13}CO-TPR run has been done in order to check the possible formation of carbon deposits upon interaction with CO. In turn, additional tests focused on analyzing the stability of the various species detected by DRIFTS during the course of the TPR run have been employed to get support for the interpretation of the various spectroscopic or CO-TPR features detected.

Experimental Section

The CeO_2 support was prepared by a reverse microemulsion method. For this, nitrate salt of Ce was introduced in a reverse microemulsion (water in oil) using *n*-heptane (Aldrich), Triton X-100 (Aldrich), and hexanol as organic solvent, surfactant, and cosurfactant, respectively. Then, this microemulsion was mixed with another similar microemulsion with diluted tetramethylammonium hydroxide (TMAH, Aldrich) in its aqueous phase in order to precipitate the cerium cations. The resulting mixture was stirred for 24 h followed by centrifugation, decanting and rinsing of the resulting solid with methanol. Finally, the solid part was dried at 110 °C for 24 h and the resulting powder was calcined under air at 500 °C for 2 h. Details of the preparation parameters employed during the synthesis of this support can be found elsewhere.[1] The same microemulsion procedure was employed to prepare a CuO reference sample. The ceria-supported CuO catalyst (with Cu wt % of 1.0) was prepared by incipient wetness impregnation of CeO_2 support using an aqueous solution of $Cu(NO_3)_2 \cdot 3H_2O$. The resulting material was dried overnight at 110 °C and subsequently calcined under air at 500 °C for 2 h. Main characteristics of the CuO/CeO_2 catalyst at structural, morphological, and electronic levels, on the basis of XRD, Raman, HRTEM-XEDS, S_{BET}, and XPS were reported elsewhere.[1] In turn, catalytic activity results on CO oxidation, CO-PROX, or WGS processes over this catalyst have been also analyzed previously.[1,6,9,10]

CO-TPR experiments employing either ^{12}CO or ^{13}CO as reductant were performed by using a Pfeiffer Omnistar mass spectrometer (MS) as detector. A DRIFTS cell (Harrick Praying Mantis) fitted with CaF_2 windows and a heating cartridge that allowed samples to be heated up to 500 °C was employed as reactor. Prior to the CO-TPR run, ca. 0.15 g of sample was calcined in situ at 500 °C under flow of 20% O_2/He for 2 h and then the sample was cooled to room temperature under the same atmosphere and extensively purged at room temperature under

* Corresponding author. E-mail: amartinez@icp.csic.es.

10.1021/jp9020504 CCC: $40.75
Published on Web 05/22/2009

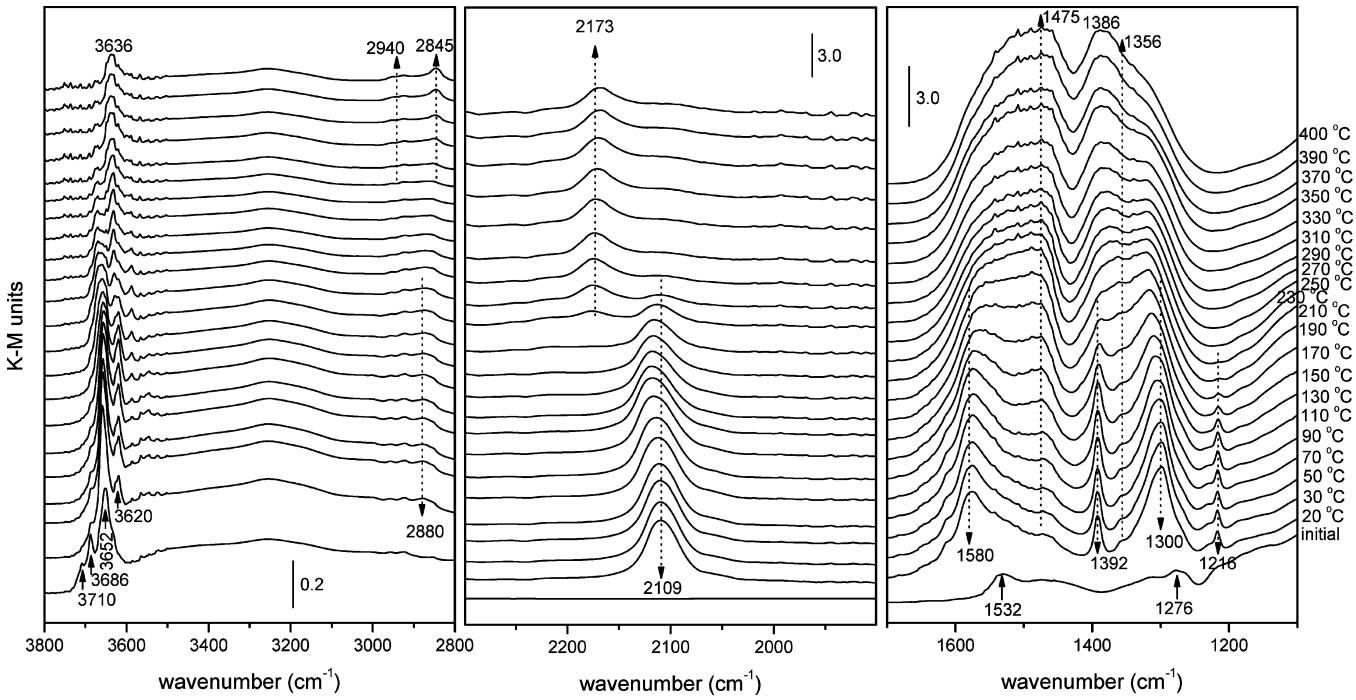

Figure 1. DRIFTS spectra recorded during ^{12}CO-TPR run over CuO/CeO_2 separated in zones where changes are detected. The bottom spectrum corresponds to the initial one recorded prior to introduction of diluted CO and the rest were recorded under diluted CO at temperatures indicated at the right. Note the CO(g) contribution has been subtracted from the spectra.

inert gas. Then, it was exposed to 5% CO/He at room temperature and, after gases equilibration, the sample temperature was raised under the CO/He atmosphere using a ramp of 10 °C min^{-1} and a flow of 50 cm^3 min^{-1}. The DRIFTS spectra were carried out using a Bruker Equinox 55 FTIR spectrometer fitted with an MCT detector. The spectra (average of 20 scans at 4 cm^{-1} resolution) were recorded typically every 20 °C. The temperature was controlled with a thermocouple in direct contact with the sample. Additional TPO−DRIFTS runs under 5% O_2/He employing a ramp of 10 °C min^{-1} were also done in some case on the catalyst subsequently to the CO-TPR run and cooling to room temperature under He. For comparison with the spectra of gaseous ^{12}CO and ^{13}CO molecules whose shape changes with the temperature as a consequence of differences in populations of rotational levels, as well as for its use as a reference for the CO-TPR tests, blank runs were done under the same conditions with inert KBr sample. The spectra taken at each temperature have been used as subtraction references in order to get rid of contribution from CO gas molecules when required for the analysis. In any case, spectra obtained in reflectance units were transformed into a form equivalent to absorption spectra by the use of the Kubelka−Munk function and referenced to those taken just before CO admission. ^{12}CO (99.95%) and ^{13}CO (99.0% purity) gases were supplied by Air Liquide and Spectra Gases, respectively. ^{13}CO contains 5% $^{13}C^{18}O$ isotope as analyzed by MS. Deconvolution of the spectra in the carbonyl region has been made by means of fitting to signals with combined Lorentzian−Gaussian line shape, taking into account the heterogeneous nature of the catalysts, employing OriginPro 7 SR4 software.

Results and Discussion

DRIFTS Characterization of Species Formed During CO-TPR Test. Figures 1 and 2 display DRIFT spectra recorded in the course of the CO-TPR tests with diluted ^{12}CO and ^{13}CO, respectively. Table 1 contains main spectral characteristics of the species detected during such tests. The spectrum of the initial sample displays bands in the highest wavenumber zone corresponding mainly to hydroxyl species. These include, on the basis of previous analyses of ceria-related materials,[11−13] isolated hydroxyls giving rise to relatively narrow bands at ca. 3712−3685 cm^{-1} (monocoordinated to surface cerium cations), as well as a series of bands or shoulders in the 3660−3520 cm^{-1} range (attributable to isolated bi- or tricoordinated species bonded on more or less unsaturated cerium cations); additionally, associated hydroxyl species giving a broad band extending from ca. 3800 to 2800 cm^{-1} are detected. Bands attributable to carbonate species of bidentate or monodentate type are detected in the 1550−1200 cm^{-1} range.[13−15] It must be noted that due to the basic character of ceria, hydroxyl and carbonate species are difficult to eliminate by the oxidizing thermal treatment, typically requiring temperatures above 750 °C which can induce an important sample sintering and surface area loss.[19,20] New carbonate-type species, all of them formed apparently over the ceria part of the catalyst in accordance with previous works of CO or CO_2 chemisorption over CeO_2,[14] are generated upon interaction of the sample with CO. Thus, bi- and mono- or poly dentate carbonates, as well as hydrogen−carbonate species, are created upon first low temperature contact with CO (Table 1). It can be noted that the hydrogen−carbonate species are formed from most basic monocoordinated hydroxyl species (band at ca. 3710 cm^{-1}), in agreement also with previous works.[13,14] In turn, formate species are formed above ca. 300 °C. Isotopic shifts observed for the carbonate-type species are in accordance with the attributions and mode assignments made (Table 1), taking also into account previous works in the literature.[13,14]

Concerning the intermediate region of the spectra, in which carbonyl species are detected, two main contributions are apparent. First, a band at ca. 2175 cm^{-1} (Figure 1), attributable to CO adsorbed on unsaturated Ce^{4+} cations (a similar band is detected when the CO-TPR run is performed over the CeO_2 support, as shown in the Supporting Information),[13] is shown

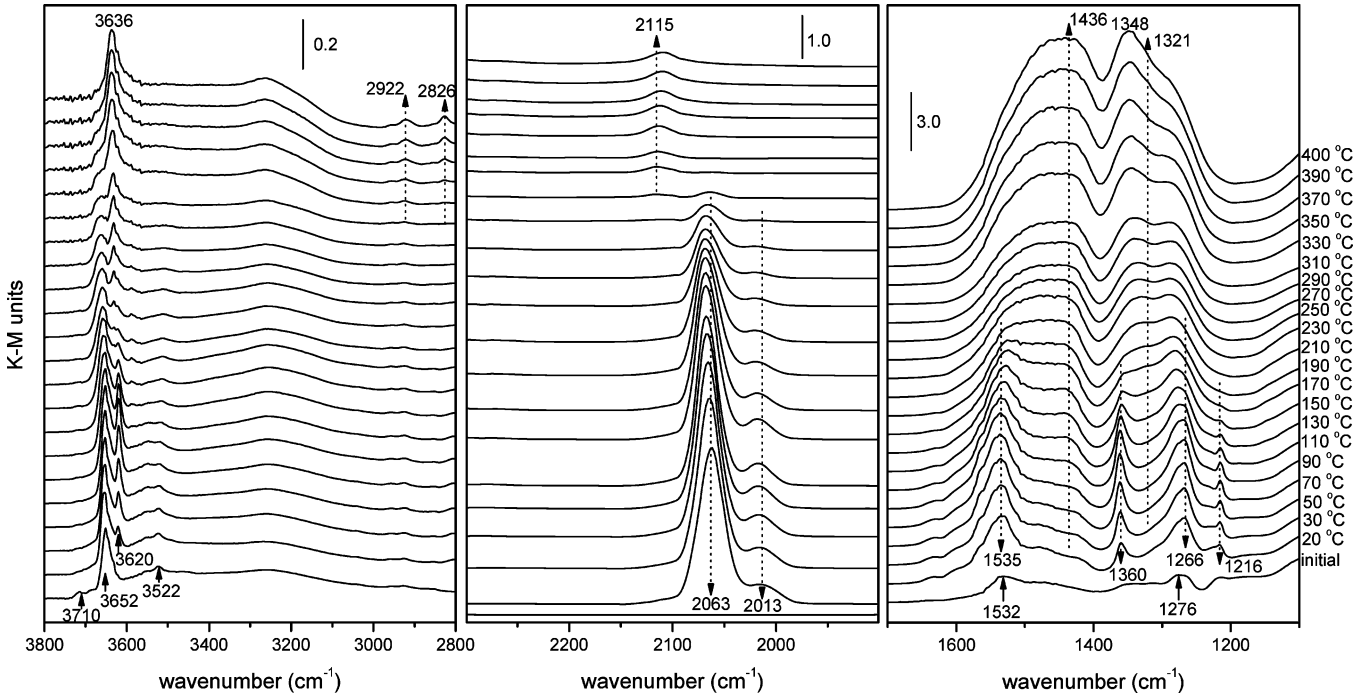

Figure 2. Same as Figure 1 for the run performed with ^{13}CO.

TABLE 1: Spectral Characteristics and Proposed Assignment of Main CO-Derived Bands Detected by DRIFTS in the Course of CO-TPR Tests over CuO/CeO_2 Catalyst

species assignment[a]	frequencies observed (cm^{-1}) and mode assignment[b]
bidentate carbonate	$\nu_{C=O}$: 1580 (1535); $\nu_{O-C-O\ (asym)}$: 1300 (1266); $\nu_{C=O} + \nu_{O-C-O\ (asym)}$: 2880 (2800)
mono- or poly dentate carbonate[c]	$\nu(CO_3^{2-})_{(asym)}$: 1475 (1436); $\nu(CO_3^{2-})_{(sym)}$: 1356 ($\approx$ 1321)
hydrogen−carbonate	$\nu_{O-C-O\ (asym)}$: $\approx$ 1600; $\nu_{O-C-O\ (sym)}$: 1392 (1360); δ_{O-H}: 1216 (1216); ν_{O-H}: 3620 (3620)
formate	$\nu_{O-C-O\ (asym)} + \delta_{C-H}$: $\approx$ 2940 (2922)[d]; ν_{C-H}: 2845 (2826); $\nu_{O-C-O\ (asym)}$: $\approx$ 1510 ($\approx$ 1460); $\nu_{O-C-O\ (sym)}$: 1386 (1348)[e]
Ce^{4+}-carbonyl	ν_{CO}: 2175−2168 (2116−2109)
Cu^{+}-carbonyl	ν_{CO}: 2117−2009 ($^{13}C^{16}O$: 2070−2062; $^{13}C^{18}O$: 2020−2012)
Cu^{+}-carbonyl[f]	ν_{CO}: 2094 ($^{13}C^{16}O$: 2052−2050; $^{13}C^{18}O$: 2004)

[a] Assignment also based on previous reports, in which further details can be also found.[1,11−13] [b] Values between parentheses correspond to resolved bands derived from $^{13}C^{16}O$ chemisorption; in the case of carbonyl species, $^{13}C^{18}O$-derived species could be also resolved and is also included between parentheses, as indicated. Mode assignment in accordance also with previous works.[12,14,15] [c] Similarities between frequencies do not allow a more definitive attribution; discussion on this can be found elsewhere.[11] [d] Mode assignment as proposed elsewhere,[12,14,16] although $\nu_{O-C-O\ (sym)}$ combination, as proposed for formate species chemisorbed on zirconia,[17,18] cannot be discarded, considering that the position of the $\nu_{O-C-O\ (asym)}$ vibration could not be fully resolved. [e] The $\nu_{O-C-O\ (sym)}$ mode is expected to be the most intense vibration in this zone although the δ_{C-H} vibration could strongly overlap.[14] [f] Tentative assignment mainly based on its relatively high stability toward treatment under inert gas flow (see text); differences between the two Cu^{+} carbonyl species are attributed to differences in respective dispersed copper oxide particle size (see text).

to be formed from 250 °C. This band is shifted from ca. 2175 to 2168 cm^{-1} (2116−2109 cm^{-1} in ^{13}CO-derived species) with increasing temperature while it displays an isotopic shift factor of ca. 1.027, somewhat higher than theoretically expected (1.023). Both facts can be related to electronic effects as a consequence of small differences in respective hydroxylation degrees, considering the important sensitivity of this species to such changes.[13] In second place, an intense band at 2109 cm^{-1}, ascribed to the Cu^{+}-carbonyl species in accordance with previous works,[1,2] is detected upon introduction of ^{12}CO at room temperature in the DRIFTS cell. Attribution of such a band to a carbonyl species is evidenced by the isotopic shift detected when ^{13}CO is employed, in which case two bands are detected at 2063 and 2013 cm^{-1}, related to chemisorption of $^{13}C^{16}O$ and $^{13}C^{18}O$, respectively, in fair agreement with theoretical isotopic shift factors (ca. 1.023 and 1.049 with respect to $^{12}C^{16}O$, respectively). The band displays a monotonous intensity decrease with increasing temperature while a slight blue shift of the band is gradually produced up to 250 °C, apparently recovering its initial position at 270 °C, above which the band practically disappears.

In turn, a close inspection of this spectral zone, by means of fitting the spectrum obtained upon introduction of CO at 20 °C (yielding maximum intensity of carbonyl species) reveals the presence of additional minor contributions as displayed in Figure 3. One of the objectives of this part of the study was related to analyzing the possibility that particular Ce^{3+} species (not necessarily reflecting the degree of reduction of the ceria component), known to give rise to a normally forbidden $^2F_{5/2}$ to $^2F_{7/2}$ electronic transition at frequencies around 2120 cm^{-1},[7,8,21] may be strongly overlapping in this region of the spectrum. Indeed, the high frequency tail of the ^{13}CO-derived spectrum could not be fully fitted by the tail of the main band at 2064 cm^{-1} (in spite of the use of flexible Lorentzian−Gaussian lines

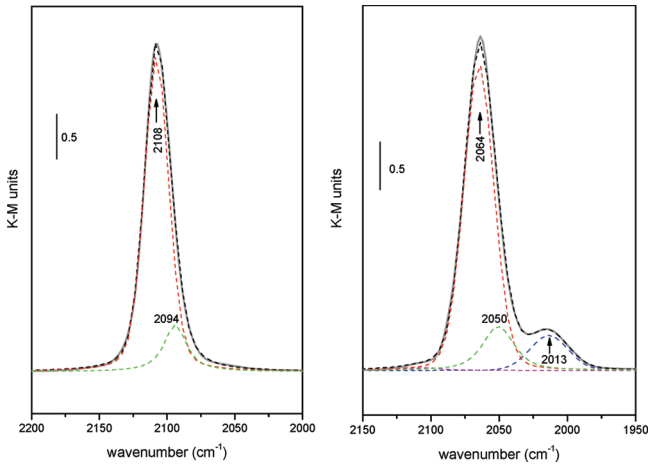

Figure 3. Deconvolution of the spectra obtained upon CO introduction at 20 °C on the CuO/CeO_2 catalyst. Left: ^{12}CO-derived. Right: ^{13}CO-derived. The corresponding CO(g) contribution at the same temperature has been subtracted in each case. The experimental spectra is shown as straight gray line while the fitting is displayed as black dashed line and the various individual contributions as dashed colored lines.

in which the ratio of Lorentzian/Gaussian contribution was not kept as fixed). Nevertheless, the mentioned tail is properly fitted by considering a small contribution at ca. 2109 cm^{-1} which accounts for the equivalent carbonyl resulting from chemisorption of the <1% ^{12}CO present in the gas (see the Experimental Section).

On the other hand, the ^{12}CO-derived spectrum could not be properly fitted with a single band. In particular, the low frequency tail requires including an additional contribution of a carbonyl species at 2094 cm^{-1} (the equivalent carbonyl at 2050 cm^{-1} in the ^{13}CO-derived spectrum also enhances the fitting in this zone of the spectrum while the residual equivalent contribution in the corresponding $^{13}C^{18}O$ zone is not required for adequate fitting). Experimental evidence for the presence of this carbonyl has been achieved in a separate set of experiments in which spectra are recorded during gradual introduction of CO in the DRIFTS cell at 20 °C (Figure 4). The spectra show that first contact with CO gives rise to exclusive formation of this carbonyl. Gradual blue shift observed with increasing contact time is consistent with the gradually increasing contribution of the carbonyl at ca. 2063 cm^{-1}, in accordance with spectra deconvolution which requires both contributions for proper fitting as well as with line width evolution detected.

Following carbonyl saturation at 20 °C (Figure 4), a final set of experiments has been focused to analyze the stability of the carbonyl species. This aims also at getting hints on the nature of the copper adsorption center. In this respect, the frequency of the copper carbonyl is often used to identify the oxidation state and structural nature of the adsorption center.[22−29] It is generally acknowledged that carbonyl bands at wavenumbers lower than ca. 2115 cm^{-1} are due to carbonyl species adsorbed on metallic copper particles while those at higher wavenumber correspond to carbonyls adsorbed on oxidized copper sites, the wavenumber increasing with the copper oxidation state. Variations in the frequency of these carbonyls have been related to changes in the nature of the exposed faces (i.e., in the degree of coordination of the copper centers). Additionally, in the case of supported catalysts, metal−support interactions must be considered as these can produce frequency shifts with respect to the values obtained on unsupported metals.[27,30−32] Indeed, Cu^+ carbonyl species have been unambiguously demonstrated

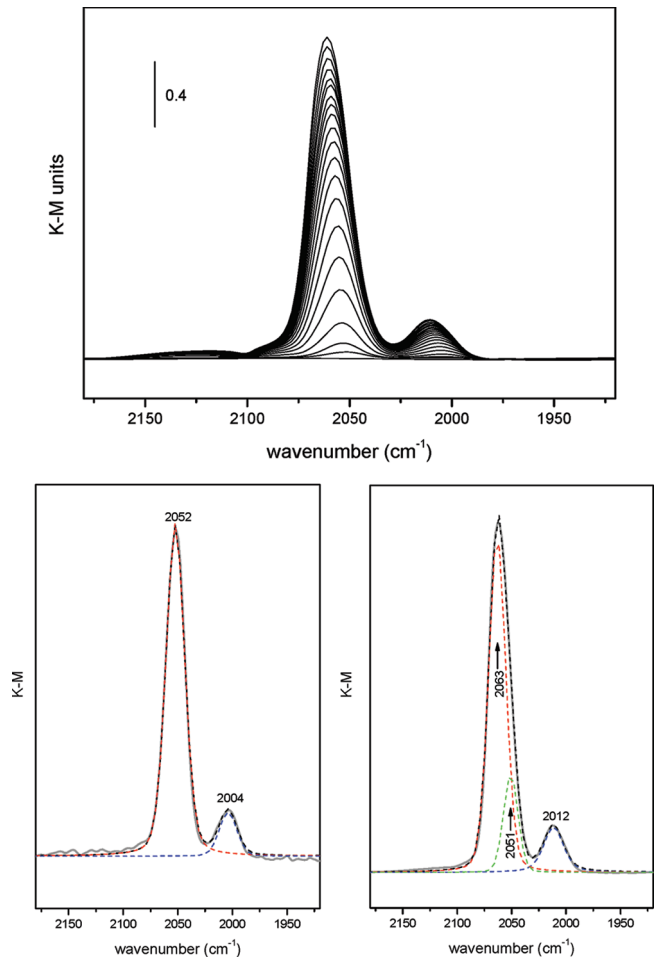

Figure 4. Top: spectra recorded during gradual introduction of ^{13}CO over CuO/CeO_2 calcined under diluted O_2 for two hours at 500 °C. For the sake of visualization, some intermediate spectra have been eliminated; the most intense one corresponds to the situation in which no further carbonyl increase was detected. Bottom: deconvolution of the spectra corresponding to the first one recorded just after CO introduction in the DRIFTS cell (left) and the final one after full equilibration (right; CO(g) bands contributions was needed to be subtracted in this latter case). The experimental spectrum is shown as straight gray line while the fitting is displayed as black dashed line and the various individual contributions as dashed colored lines.

to absorb down to 2080 cm^{-1}.[31,33−35] Therefore, an overlapping region of about 30 cm^{-1} can present overlapping Cu^0 and Cu^+ carbonyl contributions. In this respect, a typical means of identifying the nature of the adsorption centers is based on the relative strengths of the CO-copper bonds. Thus, Cu^+ carbonyls usually show significantly higher thermal stability than Cu^0 or Cu^{2+} carbonyls and hence usually withstand room temperature outgassing, while the latter would readily undergo strong desorption under the same conditions.[23,26] The band at ca. 2109 cm^{-1} in ^{12}CO-derived spectra lies at the limit of the range of frequencies, which may be assigned to carbonyls adsorbed on metallic copper particles.[22] However, the relatively high thermal resistance of these carbonyls under inert gas flow as illustrated in Figure 5 strongly suggests that the adsorption center is in an oxidized state, likely Cu^+.[27,28] It must be also noted, that practically no frequency shift is detected in this band upon carbonyl desorption (Figure 5), which indicates the absence of significant coupling effects typically found upon chemisorption on small metallic particles with heterogeneous surface structure,[22,24] in contrast to carbonyls chemisorbed on most energetically favored monocoordinated sites on pure Cu_2O.[25] In this sense,

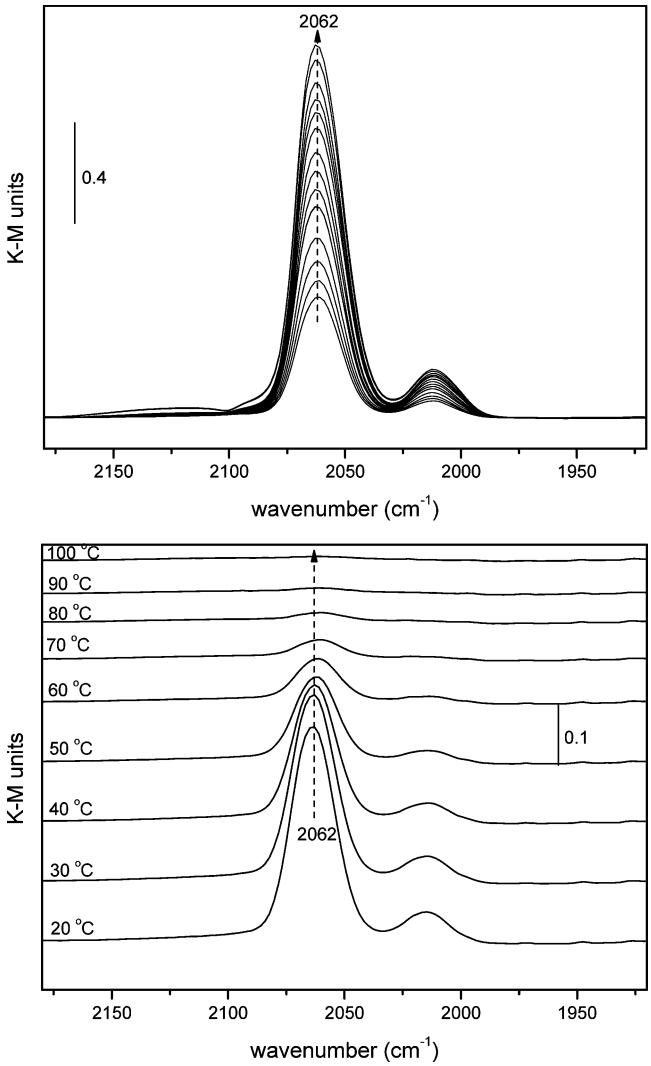

Figure 5. Top: spectra recorded during carbonyl desorption under inert gas flow at 20 °C. For the sake of visualization, some intermediate spectra have been eliminated; the less intense one corresponds to the situation in which no further carbonyl decrease was detected after prolonged treatment (ca. 60 min). Bottom: Spectra recorded upon subsequent heating under inert gas flow using a 5 °C min^{-1} ramp.

comparison between spectra in Figures 4 and 5 with similar carbonyl coverage at 20 °C validates the hypothesis done in the former paragraph in the sense that the blue shift detected upon increasing carbonyl intensity in Figure 4 must be basically related to the increase of the relative contribution of the carbonyl at 2063 cm^{-1} with respect to that at 2051 cm^{-1}. On the other hand, deconvolution fitting of the spectrum after prolonged treatment under inert gas at room temperature (not shown) suggests a relatively strong resistance of the carbonyl band at 2051 cm^{-1} toward this treatment indicating that the corresponding copper adsorption center in this case could also be tentatively ascribed to a Cu$^+$ center. These latter centers could be formed upon reduction of dispersed copper oxide clusters of relatively smaller size than dispersed copper oxide particles giving rise to the carbonyl at 2063 cm^{-1}. Such smaller copper oxide clusters are likely subjected to a stronger interaction with the ceria support, which would justify the relatively strong red shift produced in the Cu$^+$ carbonyl stretching, while they are likely more easily reduced upon interaction with CO, which would explain the higher facility for their formation evidenced by Figure 4. It must be noted that the heterogeneity in the dispersed copper oxide particles present in this catalyst is compatible with

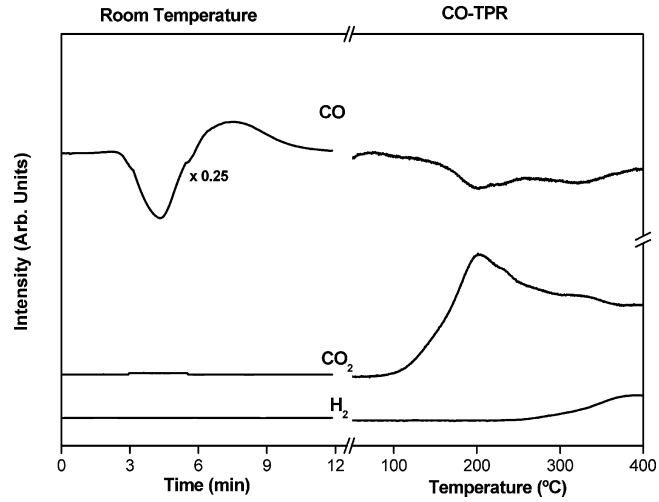

Figure 6. Evolution of gases detected over CuO/CeO$_2$ during in situ DRIFTS-MS of CO-TPR.

analysis of the CO-TPR results discussed below as well as with previous EPR and Ar$^+$-sputtering XPS exploration.[36] In any case, the relatively strong red shift detected for this type of Cu$^+$ carbonyls along with their relatively strong resistance toward outgassing suggests a strong π-back-bond component in them, according to usual σ bond-π-back-bond scheme employed to explain carbonyl bonds in this type of species.[22,25,37]

Analysis of Processes Taking Place during the CO-TPR Test. Figure 6 displays the evolution of relevant gases monitored during the CO-TPR test. First to be noted, an appreciable CO consumption without corresponding CO_2 evolution is observed already at room temperature during gases equilibration prior to starting the heating ramp, in agreement also with previous findings.[20,27] This phenomenon appears exclusive of the catalyst combining copper oxide and ceria since no room temperature CO consumption is detected when making the same experiment with the CeO_2 reference system while only a residual consumption is detected over CuO reference system under the same conditions. In principle, such low temperature consumption (ca. 4.5 cm^3 g^{-1}) could be related simply to CO chemisorption on the sample surface and/or to the existence of a more complex reduction process. According to DRIFTS spectra (Figures 1 and 2), simple chemisorption on the copper oxide component, giving rise to carbonyl species, would take place if such component is partially reduced in the starting catalyst since no band attributable to carbonyls adsorbed on Cu^{2+} species, expected to yield bands of weakly held carbonyls above 2160 cm^{-1}, typically observable only at low temperatures or high equilibrium pressures,[37] is detected. However, the possibility that the catalyst starts from a partially reduced state in the copper oxide component has been discarded on the basis of previous XPS and XANES characterization displaying both copper and cerium appear in its maximum oxidation state thermodynamically expected within the respective oxide network (as CuO and CeO_2, respectively).[1] Alternatively, CO can also chemisorb on the ceria component giving rise to carbonate species (in which case, associated formal ceria reduction is produced) when it exposes metastable surfaces like the (110), while it would only physisorb over most stable (111) faces.[38] However, no significant formation of carbonate species has been detected upon room temperature interaction of CO with the CeO_2 support (see SI), in contrast to results observed for the CuO/CeO$_2$ system (Figures 1 and 2). On the other hand, the possibility that reduction of the catalyst can occur upon CO interaction at room temperature

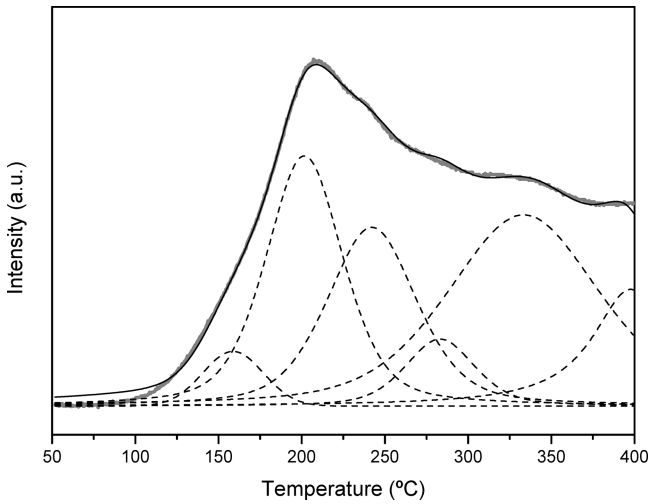

Figure 7. Deconvolution of the experimental CO_2 profile (gray thick line) obtained during CO-TPR test over CuO/CeO_2.

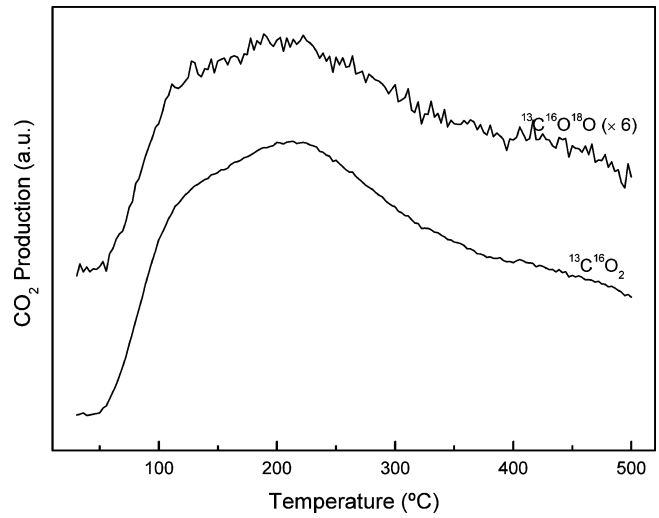

Figure 8. CO_2 evolution detected during TPO run performed subsequently to the ^{13}CO-TPR run.

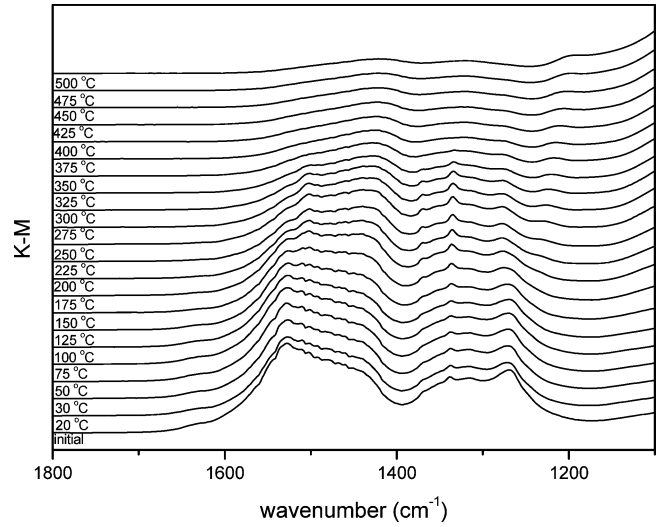

Figure 9. DRIFTS of CuO/CeO_2 in the carbonate region during TPO run subsequent to ^{13}CO-TPR, recorded at the indicated temperatures.

within a process basically involving interfacial copper oxide and ceria support sites has been evidenced by EPR and XPS in previous works;[27,28,36] indeed, about 70% of the copper has been shown to become reduced to Cu^+ species upon CO interaction at room temperature with this catalyst,[36] consistent (somewhat lower, in agreement with occurrence of a concomitant small support reduction)[27,28,36] with CO consumption detected in Figure 6. A similar process has been also proposed on the basis of TPR or TPD experiments performed over catalysts of this type.[20,39] Further proof of the existence of this reduction process is provided by the DRIFTS spectra. As displayed in Figures 1 and 2, contact with CO at 20 °C induces the simultaneous formation of Cu^+-carbonyl and carbonate species (Table 1). This evidences the existence of a redox process by which CO_2 can be formed and subsequently chemisorb in the form of carbonates over the ceria support, attribution in accordance with former infrared studies of CO_2 adsorption on pure CeO_2.[13,14]

Following CO equilibration at room temperature, the heating ramp is launched, giving rise to the profiles exhibited in the right part of Figure 6. As CO_2 profile shows a combination of several peaks, deconvolution of the CO_2 profile has been carried out to get clear insight about observed peaks in the profile which reflects six overlapping peaks (Figure 7). Thus, presence of more than one reduction peak in the catalyst instead of basically one peak in the case of pure CuO (in accordance with results in the literature)[40] is consistent with the existence of more than one copper oxide species in the present catalyst. Four intense reduction peaks at 158, 200, 241, and 282 °C along with other two peaks of lower intensity at about 333 and 398 °C are observed in the deconvoluted profile. Intense peak at 200 °C along with left shoulder peak at 158 °C have been typically referred to as α, whereas peaks at 241 and 282 °C could be assigned to β peaks (β_1 and β_2, respectively) according to the usual nomenclature employed in the scientific literature.[41,42] Such reduction temperatures are lower than that detected for pure CuO (above ca. 300 °C)[40,42] which is consistent with a ceria promotion of the massive (i.e., in addition to interfacial sites readily reduced at room temperature) reduction of the dispersed copper oxide entities.[40] In turn, the presence of the mentioned four reduction peaks is consistent with the heterogeneity in dispersed copper oxide particles discussed above. On the other hand, higher temperature peak at 333 °C is also detected in the CO_2 profile that starts at ca. 225 °C, somewhat in coincidence with observation of H_2 production (see H_2 TPR profile in Figure 6). This can be attributed to a WGS process involving interaction of CO with hydroxyls of CeO_2 still present on the surface after the pretreatment ($CO + OH^- \rightarrow CO_2 + 1/2\ H_2$ - leaving the surface reduced -). It must be noted in this sense that some CO remains in the system after 400 °C while H_2 production starts to decrease near this temperature although still remains at a relatively high level and the right tail of deconvoluted peak at 333 °C extends to temperatures higher than 400 °C (Figure 7). All these characteristic features demonstrate that the WGS process must continue above 400 °C to some extent. In our present study, DRIFTS results show that mono coordinated hydroxyl as well as hydrogen carbonate species disappear and formation of stable bi coordinated hydroxyl (3636 cm^{-1}) as well as formate species (2940, 2845, 1510, and 1386 cm^{-1}) occur at temperature higher than 200 °C during CO-TPR. All these changes in the DRIFTS spectra are accordingly related to the existence of processes like $CO + OH^- \rightarrow HCOO^-$ and $HCO_3^- + H^+ \rightarrow CO_2 + H_2O$. In this sense, deconvoluted CO_2 peak at 398 °C in Figure 7 could be related to hydrogen carbonate decomposition while some WGS reaction contribution to this peak cannot be discarded. Hydrogen carbonate decomposition is also supported by the presence of trace amount of H_2O at higher temperature (not shown in Figure 6). Therefore, MS

results obtained here are in good agreement with changes detected in the DRIFT spectra during TPR and also consistent with previous analyses on catalysts of this type.[20]

On the other hand, one of the possible processes taking place during the CO-TPR run is the disproportionation or Boudouard reaction ($2CO \rightarrow C + CO_2$) which could be produced at relatively high temperature in the presence of metallic copper;[43,44] indeed, the possibility that this type of process could take place over catalysts combining copper and ceria has been pointed out previously and could be also partially responsible of the fact that the baseline of the CO_2 profile is typically not recovered at the end of the run.[41,45,46] In order to analyze this possibility, the catalyst was subjected to TPO analysis up to 500 °C, enough to burn out possible carbon deposits formed over this type of catalysts,[47] subsequently to the CO-TPR run and after cooling under inert gas flow to room temperature. The ^{13}CO-TPR run was chosen for this purpose in order to take advantage of the fact that possible carbon deposits would in such case be related to ^{13}C species and be accordingly burnt normally as $^{13}C^{16}O_2$ while possible participation from carbonate decomposition in CO_2 evolution would include $^{13}C^{16}O_2$ but also $^{13}C^{16}O^{18}O$. As exhibited by Figure 8, CO_2 production starts around 100 °C and intense peaks are observed at ca. 130 and 225 °C. Fairly similar profiles are detected for $^{13}C^{16}O_2$ and $^{13}C^{16}O^{18}O$, indicating that CO_2 evolution is basically related to carbonate decomposition, as supported also by DRIFTS spectra (Figure 9).

Conclusions

In situ DRIFTS-MS studies of interaction of ^{12}CO and ^{13}CO with CuO/CeO_2 catalyst allow unambiguous assignment of the various carbonyl and carbonate-type species formed and a complete analysis of processes taking place during CO-TPR tests. A reduction process taking place already upon CO interaction at room temperature is evidenced by the simultaneous formation of Cu^+ carbonyl and carbonate species (as evident by DRIFTS) and consumption of CO (as evident by MS). In addition to steps related mainly to reduction of the copper oxide component in the catalyst, the WGS reaction is revealed to take place upon interaction of CO with surface hydroxyl groups above ca. 275 °C, while occurrence of the Boudouard reaction appears only residual during the CO-TPR run up to 400 °C, on the basis of TPO analysis performed subsequently to the ^{13}CO-TPR test.

Acknowledgment. P.B. is thankful to 6th European Community Framework Program for a Marie Curie Incoming International Fellowship. A.L.C. and A.H. thank the CSIC and MICINN for JAE and FPU PhD grants, respectively, under which this work was carried out. Financial support by MEC Plan Nacional (project CTQ2006-15600/BQU) and Comunidad de Madrid (project ENERCAM S-0505/ENE/000304) is acknowledged.

Supporting Information Available: Additional DRIFTS spectra. This material is available free of charge via the Internet at http://pubs.acs.org.

References and Notes

(1) Gamarra, D.; Munuera, G.; Hungría, A. B.; Fernández-García, M.; Conesa, J. C.; Midgley, P. A.; Wang, X. Q.; Hanson, J. C.; Rodriguez, J. A.; Martínez-Arias, A. *J. Phys. Chem. C* **2007**, *111*, 11026, and references therein.

(2) Gamarra, D.; Belver, C.; Fernández-García, M.; Martínez-Arias, A. *J. Am. Chem. Soc.* **2007**, *129*, 12064.

(3) Wang, X.; Rodriguez, J. A.; Hanson, J. C.; Gamarra, D.; Martínez-Arias, A.; Fernández-García, M. *J. Phys. Chem. B* **2006**, *110*, 428, and references therein.

(4) Luo, M.-F.; Song, Y.-P.; Lu, J.-Q.; Wang, X.-Y.; Pu, Z.-Y. *J. Phys. Chem. C* **2007**, *111*, 12686.

(5) Zhou, R.-X.; Yu, T.-M.; Jiang, X.-Y.; Chen, F.; Zheng, X.-M. *Appl. Surf. Sci.* **1999**, *148*, 263.

(6) Gamarra, D.; Hornés, A.; Koppány, Z.; Schay, Z.; Munuera, G.; Soria, J.; Martínez-Arias, A. *J. Power Source* **2007**, *169*, 110.

(7) Binet, C.; Badri, A.; Lavalley, J.-C. *J. Phys. Chem.* **1994**, *98*, 6392.

(8) Daly, H.; Ni, J.; Thompsett, D.; Meunier, F. C. *J. Catal.* **2008**, *254*, 238.

(9) Wang, X.; Rodriguez, J. A.; Hanson, J. C.; Gamarra, D.; Martínez-Arias, A.; Fernández-García, M. *J. Phys. Chem. B* **2006**, *110*, 428.

(10) Martínez-Arias, A.; Hungría, A. B.; Munuera, G.; Gamarra, D. *Appl. Catal., B* **2006**, *65*, 207.

(11) Laachir, A.; Perrichon, V.; Badri, A.; Lamotte, J.; Catherine, E.; Lavalley, J. C.; El Fallah, J.; Hilaire, L.; Le Normand, F.; Quéméré, E.; Sauvion, G. N.; Touret, O. *J. Chem. Soc., Faraday Trans.* **1991**, *87*, 1601.

(12) Badri, A.; Binet, C.; Lavalley, J.-C. *J. Chem. Soc., Faraday Trans.* **1996**, *92*, 4669.

(13) Binet, C.; Daturi, M.; Lavalley, J.-C. *Catal. Today* **1999**, *50*, 207.

(14) Li, C.; Sakata, Y.; Arai, T.; Domen, K.; Maruya, K.-I.; Onishi, T. *J. Chem. Soc., Faraday Trans. 1* **1989**, *85*, 929.

(15) Hadjiivanov, K. I.; Vayssilov, G. N. *Adv. Catal.* **2002**, *47*, 307.

(16) Li, C.; Sakata, Y.; Arai, T.; Domen, K.; Maruya, K.; Onishi, T. *J. Chem. Soc., Faraday Trans. 1* **1989**, *85*, 1451.

(17) Hadjiivanov, K. I.; Korhonen, S. T.; Calatayud, M.; Krause, A. O. I. *J. Phys. Chem. C* **2008**, *112*, 16096.

(18) Busca, G.; Lamotte, J.; Lavalley, J. C.; Lorenzelli, V. *J. Am. Chem. Soc.* **1987**, *109*, 5197.

(19) Trovarelli, A., Ed.; *Catalysis by Ceria and Related Materials*; Imperial College Press: London, 2002.

(20) Caputo, T; Lisi, L; Pirone, R.; Russo, G. *Appl. Catal., A* **2008**, *348*, 42.

(21) Meunier, F. C.; Reid, D.; Goguet, A.; Shekhtman, S.; Hardacre, C.; Burch, R.; Deng, W.; Flytzani-Stephanopoulos, M. *J. Catal.* **2007**, *247*, 277.

(22) Hollins, P. *Surf. Sci. Rep.* **1992**, *16*, 53.

(23) Padley, M. B.; Rochester, C. H.; Hutchings, G. J.; King, F. *J. Catal.* **1994**, *148*, 438.

(24) Kohler, M. A.; Cant, N. W.; Wainwright, M. S.; Trimm, D. L. *J. Catal.* **1989**, *117*, 188.

(25) Scarano, D.; Bordiga, S.; Lamberti, C.; Spoto, G.; Ricchiardi, G.; Zecchina, A.; Otero Areán, C. *Surf. Sci.* **1998**, *411*, 272.

(26) Topsøe, N.-Y.; Topsøe, H. *J. Mol. Catal. A* **1999**, *141*, 95.

(27) Martínez-Arias, A.; Fernández-García, M.; Soria, J.; Conesa, J. C. *J. Catal.* **1999**, *182*, 367.

(28) Martínez-Arias, A.; Fernández-García, M.; Gálvez, O.; Coronado, J. M.; Anderson, J. A.; Conesa, J. C.; Soria, J.; Munuera, G. *J. Catal.* **2000**, *195*, 207.

(29) Coloma, F; Marquez, F.; Rochester, C. H.; Anderson, J. A. *Phys. Chem. Chem. Phys.* **2000**, *2*, 5320.

(30) Lokhov, Yu. A.; Sadykov, V. A.; Tikhov, S. F.; Popovskii, V. V. *Kinet. Katal.* **1985**, *26*, 177.

(31) Davydov, A. A. *Kinet. Katal.* **1985**, *26*, 157.

(32) Bensalem, A.; Muller, J.-C.; Tessier, D.; Bozon-Verduraz, F. *J. Chem. Soc., Faraday Trans.* **1996**, *92*, 3233.

(33) Busca, G. *J. Mol. Catal.* **1987**, *43*, 225.

(34) Huang, Y. Y. *J. Am. Chem. Soc.* **1973**, *95*, 6636.

(35) Howard, J.; Nicol, J. M. *J. Chem. Soc. Faraday Trans. 1* **1989**, *85*, 1233.

(36) Martínez-Arias, A; Hungría, A. B.; Fernández-García, M.; Conesa, J. C.; Munuera, G. *J. Phys. Chem. B* **2004**, *108*, 17983.

(37) Hadjiivanov, K. I.; Kantcheva, M.; Klissurski, D. G. *J. Chem. Soc. Faraday Trans.* **1996**, *92*, 4595.

(38) Huang, M.; Fabris, S. *J. Phys. Chem. C* **2008**, *112*, 8643.

(39) Avgouropoulos, G.; Ioannides, T. *Catal. Lett.* **2007**, *116*, 15.

(40) Avgouropoulos, G.; Ioannides, T. *Appl. Catal., A* **2003**, *244*, 155.

(41) Papavasiliou, J.; Avgouropoulos, G.; Ioannides, T. *Catal. Commun.* **2004**, *5*, 231.

(42) Bera, P; Priolkar, K. R.; Sarode, P. R.; Hegde, M. S.; Emura, S.; Kumashiro, R.; Lalla, N. P. *Chem. Mater.* **2002**, *14*, 3591.

(43) Jagannathan, K.; Srinivasan, A.; Hegde, M. S.; Rao, C. N. R. *Surf. Sci.* **1980**, *99*, 309.

(44) van Daelen, M. A.; Li, Y. S.; Newsam, J. M.; van Santen, R. A. *Chem. Phys. Lett.* **1994**, *226*, 100.

(45) Valdés-Solís, T.; Marbán, G.; Fuertes, A. B. *Catal. Today* **2006**, *116*, 354.

(46) Martínez-Arias, A.; Cataluña, R.; Conesa, J. C.; Soria, J. *J. Phys. Chem. B* **1998**, *102*, 809.

(47) Liang, Q.; Wu, X.; Weng, D.; Lu, Z. *Catal. Commun.* **2008**, *9*, 202.

JP9020504